ECCOMAS Congress 2016
VII European Congress on Computational Methods in Applied Sciences and Engineering
M. Papadrakakis, V. Papadopoulos, G. Stefanou, V. Plevris (eds.)
Crete Island, Greece, 5–10 June 2016

EXPERIMENTAL VALIDATION OF A MODEL UPDATE PROCEDURE FOCUSING ON SMALL GEOMETRIC DEVIATIONS

Thomas Maywald[1], **Arnold Kühhorn**[1] **and Sven Schrape**[2]

[1] Brandenburg University of Technology (BTU)
Siemens-Halske-Ring 14
D-03046 Cottbus, Germany
e-mail: {thomas.maywald,kuehhorn}@b-tu.de

[2] Rolls-Royce Deutschland Ltd & Co KG
Eschenweg 11
D-15827 Blankenfelde-Mahlow, Germany
e-mail: sven.schrape@rolls-royce.com

Keywords: Model Update, Mesh Morphing, Model Validation, Vibration Measurements, Geometric Mistuning, Blisk Vibrations.

Abstract. *This contribution presents a model update procedure and its experimental validation using the example of a blade integrated disk rotor. This so called blisk is discretized using the finite element method. It is well known that numerical blisk models based on the ideal tuned design show major differences in structural dynamic behavior compared to the real rotor. In this context a modification of the mechanical simulation model should lead to a better accordance of numerical results and the real blisk characteristics. The described model update procedure utilizes data of an optical 3D measurement system. Using this data enables to identify geometric deviations between the ideal design and its real counterpart. Within the update procedure the originally tuned finite element mesh is modified in order to match the measured geometry of the real part. This is done by defining several morph regions. The outer surface nodes of these morph regions change their position along the surface normal vector until they meet the defined deviation constraint. Based on eigenvalue calculations employing free boundary conditions the sensitivity of structural dynamic behavior is shown with respect to small geometric changes. Finally computed eigenvalues and eigenvectors of the updated simulation model are compared with vibration measurement data. A laser Doppler vibrometer is used to detect the vibration responses of the impact excited structure. All experiments are carried out under technical vacuum conditions in order to minimize ambient air damping. In the context of an experimental modal analysis this low damping condition helps to identify more natural frequencies of the investigated structure. This leads to a much more efficient model validation.*

1 INTRODUCTION

One of the main objectives in engineering practice is to predict structural behavior due to different load conditions. There are several possibilities reaching this target. One of the most popular ways to simulate mechanical systems behavior is to discretize a structure using the Finite Element Method (FEM). The transformation of a continuum into finite elements is accompanied by several challenges. On the one hand this discretization necessarily leads to differences between the CAD geometry of a part and its simulation model. On the other hand the manufactured part is affected by errors. That means that there are deviations between the digitally designed CAD model and its real counterpart. Commonly deviations between a simulation model and the real mechanical system cause an inaccurate prediction of structural behavior. Therefore several model update strategies are available in order to harmonize numerical prediction with experimental experiences.

This contribution presents a model update procedure which focuses on small manufacturing driven geometry changes of a rotating aircraft engine part. Object of investigation is a blade integrated disk rotor (blisk). Here, the milling process causes small geometric deviations between real part and the designed rotor. These deviations from the ideal design intention, known as 'mistuning', come along with a number of particularities in structural dynamics. Thus, mistuning can cause localized mode shapes which lead to a concentration of vibration energy in several or even a single blade [1-5]. By this the regular character of the mode shapes gets lost. In presence of a dynamic load case these blades are subject to higher magnitudes of vibration induced stresses compared to the ideal design.

Traditionally these mistuning effects are taken into account by a stiffness proportional model update approach [6-9]. The central point of this strategy is to modify the Young's modulus or respectively the stiffness matrix of each rotor blade until the finite element model is able to predict measured natural frequencies of the real rotor blade. It has been shown by a number of researchers that this is a sufficient way to simulate mistuning effects [6-9]. The advantage of this method is that there is only one model update parameter per blade. Therefore this model modification is easy to handle and no extensive computational resources are needed. Unfortunately, comprehensive measurements are necessary to identify the mistuned natural frequencies of the real system which must be known for model update. Furthermore the reliability of this stiffness proportional approach is limited to a comparatively small frequency range. This means the model update has to be done separately for each frequency range of interest.

Especially these disadvantages motivate the community to look for alternative ways of model update. A promising approach of the recent past is to consider the geometric deviations due to manufacturing within the simulation model. Existing publications dealing with this topic clearly indicate the relationship between geometry deviations and simulation model dynamics [10-12]. But finally a validation of the methodology turned out to be difficult due to the small manufacturing tolerances which have to be modeled. For this reason the present paper discusses an updated model of an industrial test blisk which could be validated for a comparatively large frequency range.

2 IDEALIZED STRUCTURAL DYNAMICS

To get a first impression of structural dynamics behavior the modal parameters of the initial rotor design has to be determined. The homogeneous equation of motion reads:

$$M\ddot{x}(\mathrm{t}) + D\dot{x}(\mathrm{t}) + Kx(\mathrm{t}) = 0. \tag{1}$$

Herein M represents the mass matrix, D the structural damping matrix and K the stiffness matrix of the blade integrated disk. Further on an undamped system is assumed ($D = 0$). The assumption results from knowledge of modal structural damping ratios of those structures which are considerably lower than $\zeta = 0.3\%$ [13, 14]. The influence of those structural damping values is negligibly in case of free blisk vibrations. Consequently the modal parameters sought for could be identified by formulating and solving the undamped eigenvalue problem

$$(M\lambda_k^2 + K)\varphi_k e^{\lambda_k t} = 0\,, \tag{3}$$

where λ_k is the k-th eigenvalue and φ_k is the k-th eigenvector of the system. To compute the needed system matrices M and K a finite element mesh has to be created. Figure 1 shows the finite element mesh for one sector with about 53.500 continuum elements of type C3D10.

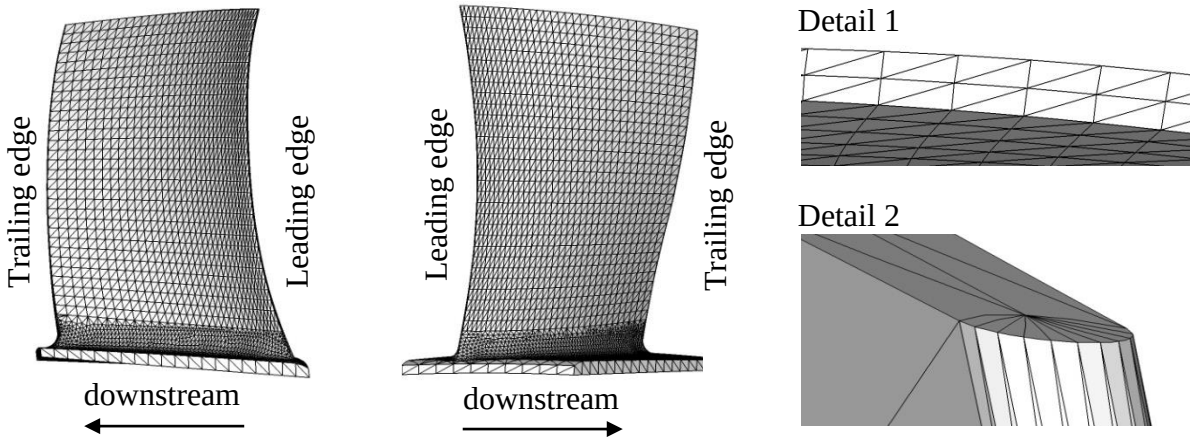

Figure 1: Finite element sector mesh of a blade integrated disk rotor (disk mesh not shown)

Two elements were used in blade thickness direction (Figure 1, Detail 1). The Leading edge curve is discretized through 12 nodes and the trailing edge curve through 21 nodes (Figure 1, Detail 2). Because all sectors are identical for the tuned design intention the modal parameters of the whole rotor were calculated by using a single sector model with cyclic symmetry boundary conditions. Figure 2 illustrates the first three computed mode shapes whose displacements are located at the blade section of the rotor.

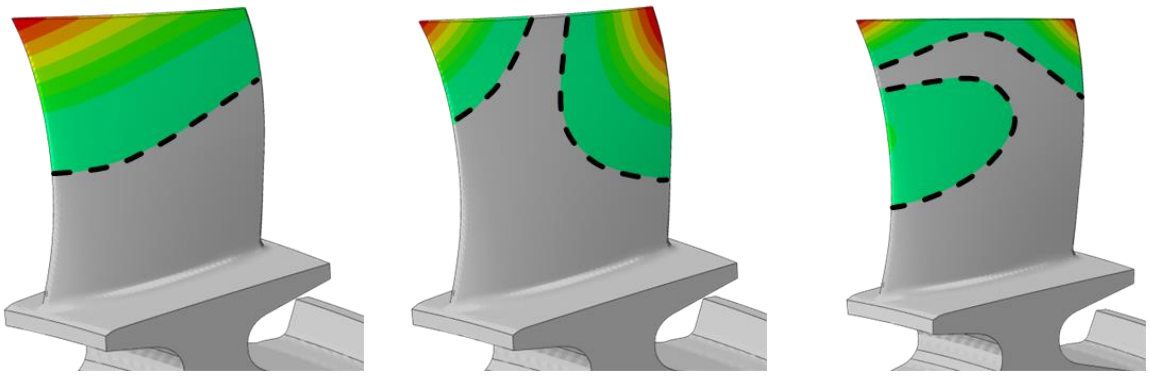

Blade mode 1 Blade mode 2 Blade mode 3

Figure 2: Computed blade mode shapes of the tuned simulation model with cyclic symmetry boundary conditions

Furthermore the vibration modes of the tuned model are categorized according to three major criteria. The cyclic symmetry mode index (CSM), the distribution of strain energy as well as the mode shape similarity are considered in order to arrange all resonances up to $f_{norm} = 4.5$ in a nodal diameter map shown in Figure 3. The maximum cyclic symmetry mode index, that can occur, is limited by the number of blades N. In case of an even number of blades it is given by

$$\mathrm{CSM}_{\max} = \frac{\mathrm{N}}{2}, \tag{4}$$

for an odd number of blades follows

$$\mathrm{CSM}_{\max} = \frac{\mathrm{N}-1}{2}. \tag{5}$$

Secondly a mode classification according to blade-dominated, disk-dominated or mixed mode is done by the assessment of the strain energy distribution as introduced in [15]. A strain energy localization of more than 86% within the blade region indicates a blade dominated mode. Accordingly a disk dominated mode is characterized by 75 % strain energy localization inside the disk. The remaining modes are summarized as mixed modes. These limits are problem specific values and may vary for different blisk applications.

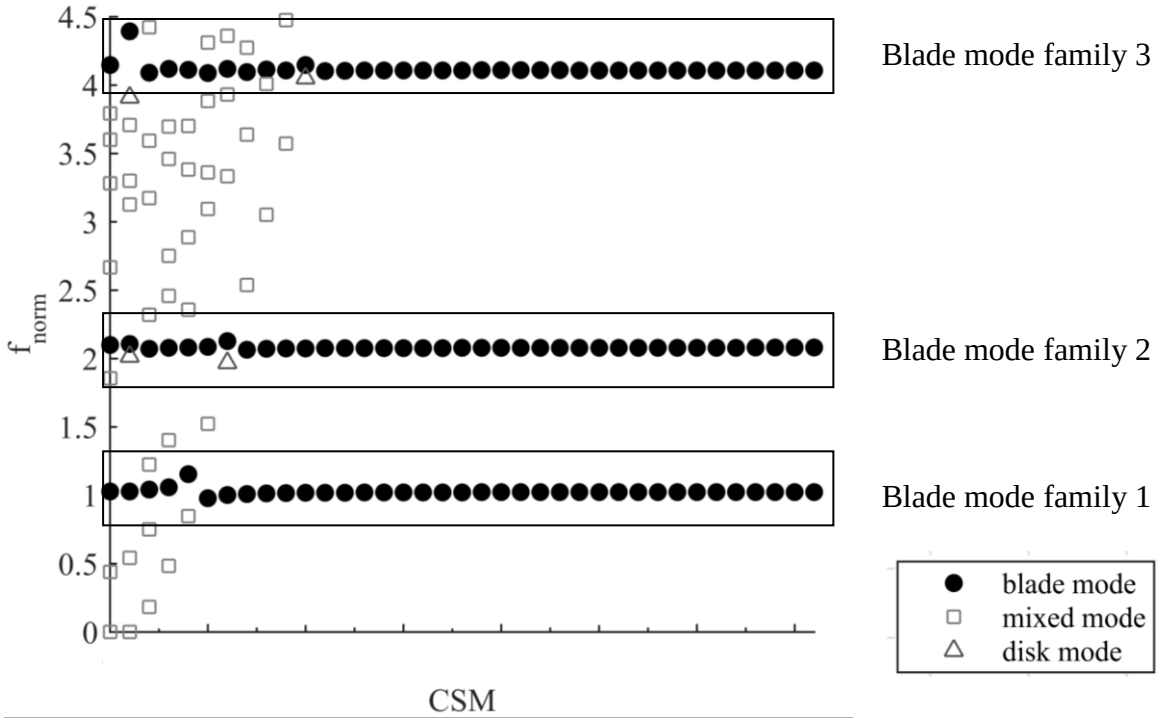

Figure 3: Nodal diameter plot

In a last step groups of classified modes with almost the same blade mode shape are identified by using the Modal Assurance Criterion (MAC) as explained in [16]. At this point several cyclic symmetry modes with similar or nearly the same blade mode shapes (MAC > 0.9) establish a family of modes. Inside Figure 3 the identified blade mode families are highlighted by a rectangle.

3 MODEL UPDATE PROCEDURE

As described in the introduction the manufacturing process always causes deviations between the ideal design intention and the real part. Considering these differences is of major importance in order to compute structural dynamics characteristics as accurate as possible. A two step procedure is needed to improve the ideal simulation model of the blade integrated disk described in chapter 2.

First of all the real geometry of the part has to be digitalized. To get the requested high resoluted surface information an optical 3D geometry measurement system is used as shown in Figure 4.

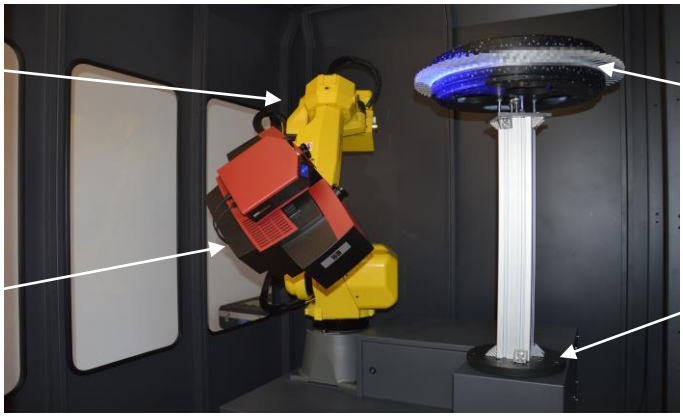

Figure 4: Non contact geometric measurement system of TU Dresden - Chair of Turbomachinery and Flight Propulsion

These high resolution measuring cameras are well proven in engineering practice and represent a state of the art measurement solution for reversed engineering. Precision of such a system has been proven to be within 2.5 µm [17]. One major advantage of such a non contact solution is the possibility to get a large number of coordinate informations very fast. Furthermore this technology allows capturing coordinates from areas which are difficult to access and could not be taken into account using conventional coordinate measurement machines. More details, advantages and disadvantages concerning optical coordinate measurements are published in [17-19]. The experimental setup which was used to get the results presented in the following includes an optical scan head, a robot arm for moving the scan head automatically and a rotatable table that carries the test blisk.

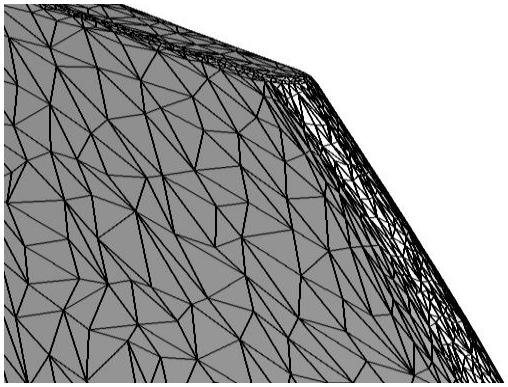

Figure 5: Triangulated surface based on optical measurements in the tip area of an exemplary trailing edge

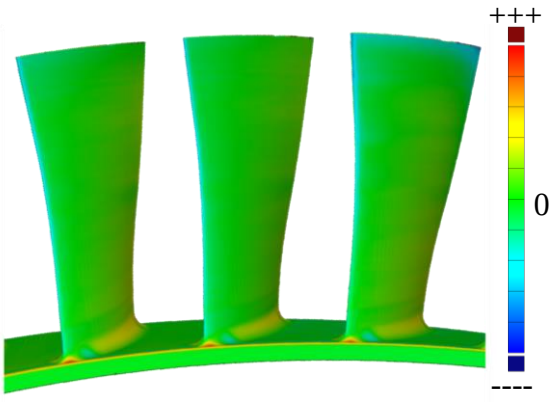

Figure 6: Deviation plot for an exemplary blade ring section - initial finite element mesh versus measured part geometry

After digitalizing the blisk the resulting point cloud data were processed to a triangulated surface mesh of the blisk shown in Figure 5. Due to experimental setup restrictions it is not possible to scan the disk of the part as well. Because of that the following data evaluation focuses on the blade ring (Figure 6). The deviations between tuned design and the real part are quantified by calculating the normal to surface distances for every node of the surface mesh. As shown in Figure 6 the deviations remain in lower triple digit micro meter range (triple + or triple −). Positive or respectively negative values indicate additional or missing material. Large deviations are mainly identified in blade leading, tip and trailing edge region. The green color indicates that the mean error of the remaining blade regions is much lower in the single digit micrometer range.

Within the second step of the model update procedure the finite element mesh has to be modified in order to match the experimentally identified surface mesh. The mesh modification shape is calculated evaluating the deviations for each mesh node of the reference mesh (Figure 1) along its element normal. The shape illustrated in Figure 7 is used to modify the initial finite element mesh (Figure 1) to ensure the best representation of the measured surface (Figure 5). Each node is shifted along its shape vector. A penetration of the measured surface mesh is not permitted in this context.

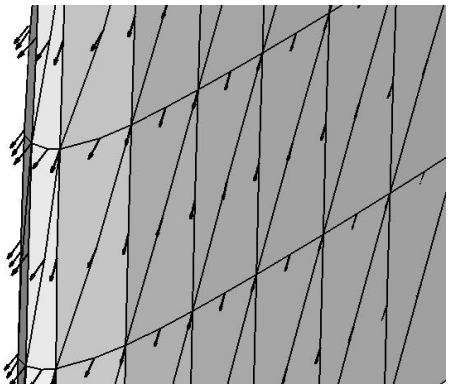

Figure 7: Mesh modification shape for exemplary leading edge

Figure 8: Deviation plot for a an exemplary blade ring section - updated finite element mesh versus measured part geometry

After finishing mesh morphing the updated model has to be compared with the measured part geometry. The corresponding deviation plot (Figure 8) shows nearly no visible differences between updated mesh and measured real part. On average the remaining deviations are in range of plus minus one digit micrometer. For this reason model modification is assessed to be sufficient.

4 MODEL VALIDATION METHOD

The mesh updating procedure presented in Chapter 3 affects both the calculated mass matrix of the investigated structure and the stiffness matrix. Compared to Chapter 2 the originally assumed cyclic symmetry of the blisk is disturbed due to the introduced geometric modifications. Commonly there is an influence on the resulting modal parameters evaluated by solving the undamped eigenvalue problem as described in Equation 3. These updated modal characteristics have to be checked for validity. Commonly modal parameters of the real part are identified by an experimental modal analysis and compared to their numerical counterparts. As shown in Figure 3 natural frequencies of a blade integrated disk are appearing very close to each other. Therefore the comprehensive natural frequency identification is dif-

ficult due to modal coupling effects. For this reason a vacuum test stand is used in order to minimize ambient air damping. In an experimental modal analysis this low damping condition helps to identify more natural frequencies of the investigated structure since modal coupling is decreasing.

4.1 Experimental Setup

The experimental determination of modal parameters within low pressure condition is carried out inside a vacuum test stand (Figure 9). Vibration excitation is realized with an impact mechanism. In addition laser scanning vibrometer measurements are applied to determine one frequency response function per blade in the frequency range of the blade modes 1 to 3 (Figure 3). A foam cuboid is used to support the blisk and ensure nearly free boundary conditions. Disturbing acoustical resonances are prevented by facing the inner surface of the chamber with nubby foam material.

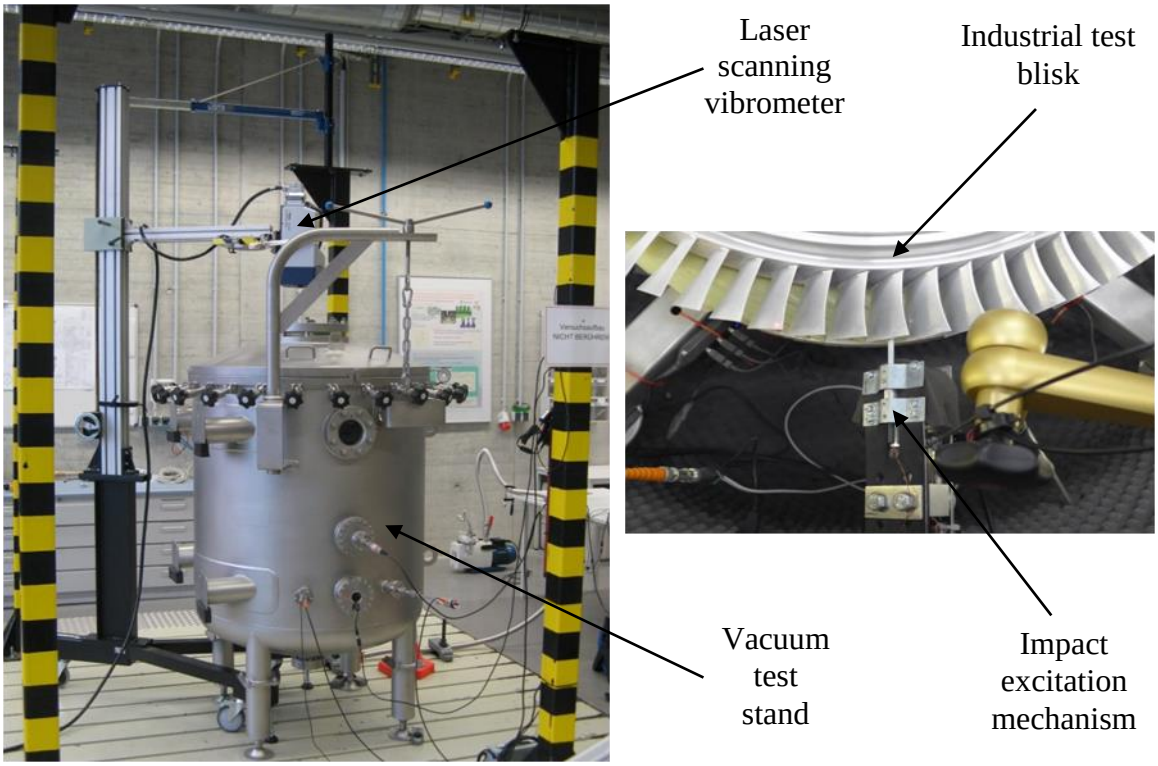

Figure 9: Vacuum test stand and experimental setup in detail

After initializing the test setup the ambient air pressure inside the vacuum champer is reduced to 100 Pa. Vibration measurements are carried out for all blades of the blisk successively at the leading edge tip (Figure 10). The location of impact does not change during the experiments.

To illustrate the influence of low pressure conditions on measured vibration response Figure 11 compares the normalized measured vibration velocity for an exemplary blade at 100 Pa and 100 kPa respectively. Apart from ambient pressure all experimental parameters remain unchanged. As already mentioned vacuum condition largly eliminates damping contribution of the surrounding fluid and results to a more gently decreasing amplitude response in time domain. Measurement data exemplary shown demonstrate that even if the damping contribution of the surrounding air is low it has major influence on system response. In order to emphasize the importance of this low damping condition for modal parameter identification the

time signal shown in Figure 11 is converted into frequency domain using a Fast Fourier Transformation within the next step.

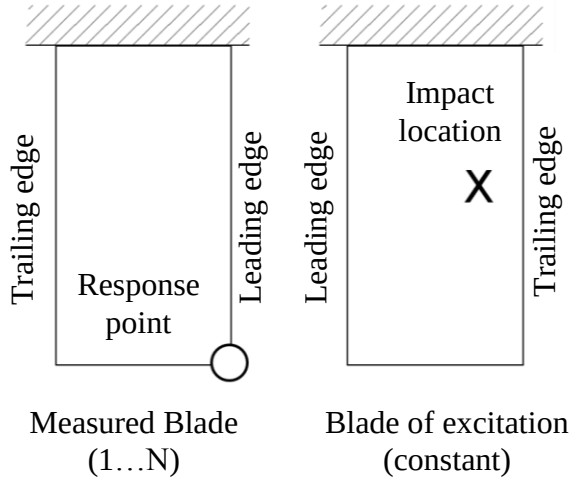

Figure 10: Experimental setup – location of response measurement (left) and impact excitation (right)

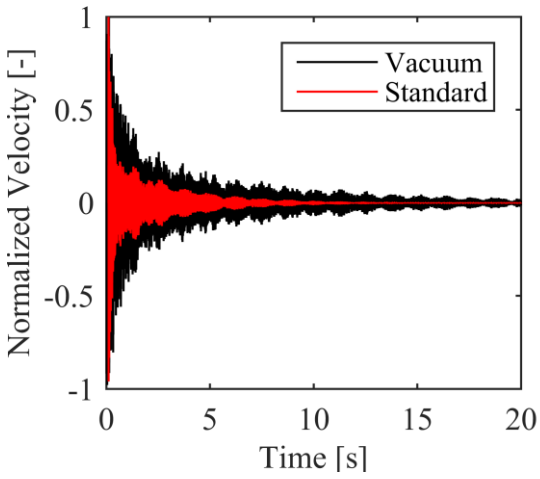

Figure 11: Comparison of normalized impact response at vacuum (100 Pa) and at ambient air pressure (100 kPa) for an exemplary blade

A detailed look at the results of this transformation (Figure 12) clarifies that decreasing ambient pressure affects a better separation of resonance peaks in frequency domain. Furthermore a small frequency shift appears due to modified damping values (cf. Equation 2). The Phase spectrum illustrated in Figure 13 confirms the impression of better identification opportunities at vacuum conditions.

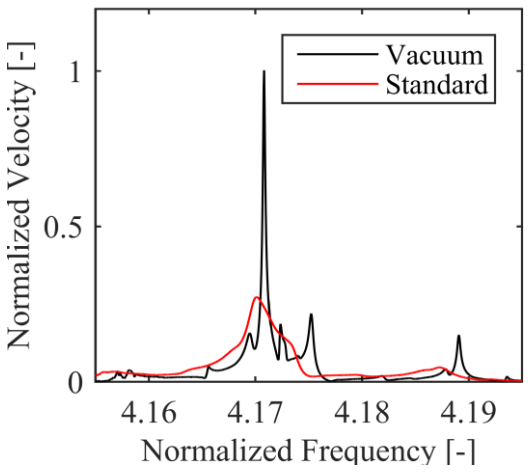

Figure 12: Comparison of normalized velocity spectrum at vacuum (100 Pa) and at ambient air pressure (100 kPa) for an exemplary blade

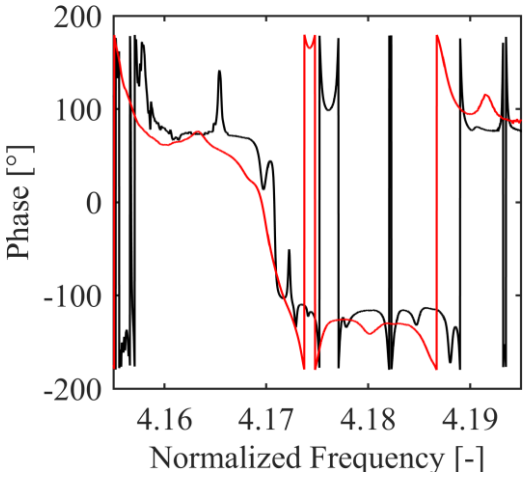

Figure 13: Comparison of phase spectrum at vacuum (100 Pa) and at ambient air pressure (100 kPa) for an exemplary blade

In context of a sufficient model validation it is advantageous to identify as much modal parameters as possible by an experimental modal analysis. The blade integrated disk considered here has extremely strong coupled resonance frequencies. Because of that the presented test facility helps to realize an effective simulation model validation.

4.2 Modal Parameter Identification

Within the next step model parameters have to be extracted from measurement data received by impact measurements described in Chapter 4.1. There are a number of publications dealing with modal parameter identification from vibration experiments. Due to strong coupled resonances as mentioned in the chapter before a multi degree of freedom approach (MDOF) is necessary for interpreting measurement results. The procedure applied here uses an optimization-aided nonlinear least square method in order to fit the frequency response function. A detailed description of this method is given in [20].

Figure 14 shows an exemplary frequency response function fit. Illustrated are the velocity and phase spectra resulting from the experiment (black) and fitted with the MDOF approach (red) in the frequency range of blade mode 1 (cf. Figure 3). Additionally the residuals are defined by

$$\mathrm{Error(f)} = \frac{\left|\mathrm{H}_1^{\mathrm{fit}} - \mathrm{H}_1^{\mathrm{exp}}\right|}{\left|\mathrm{H}_1^{\mathrm{exp}}\right|}. \tag{6}$$

Herein H_1 denotes the complex frequency response function. Amplitude and phase error are plotted separately on the top of Figure 14. Close to resonances the fitting error is in low one digit percentage range. Thus, a reliably natural frequency, damping value and eigenvector identification can be guaranteed.

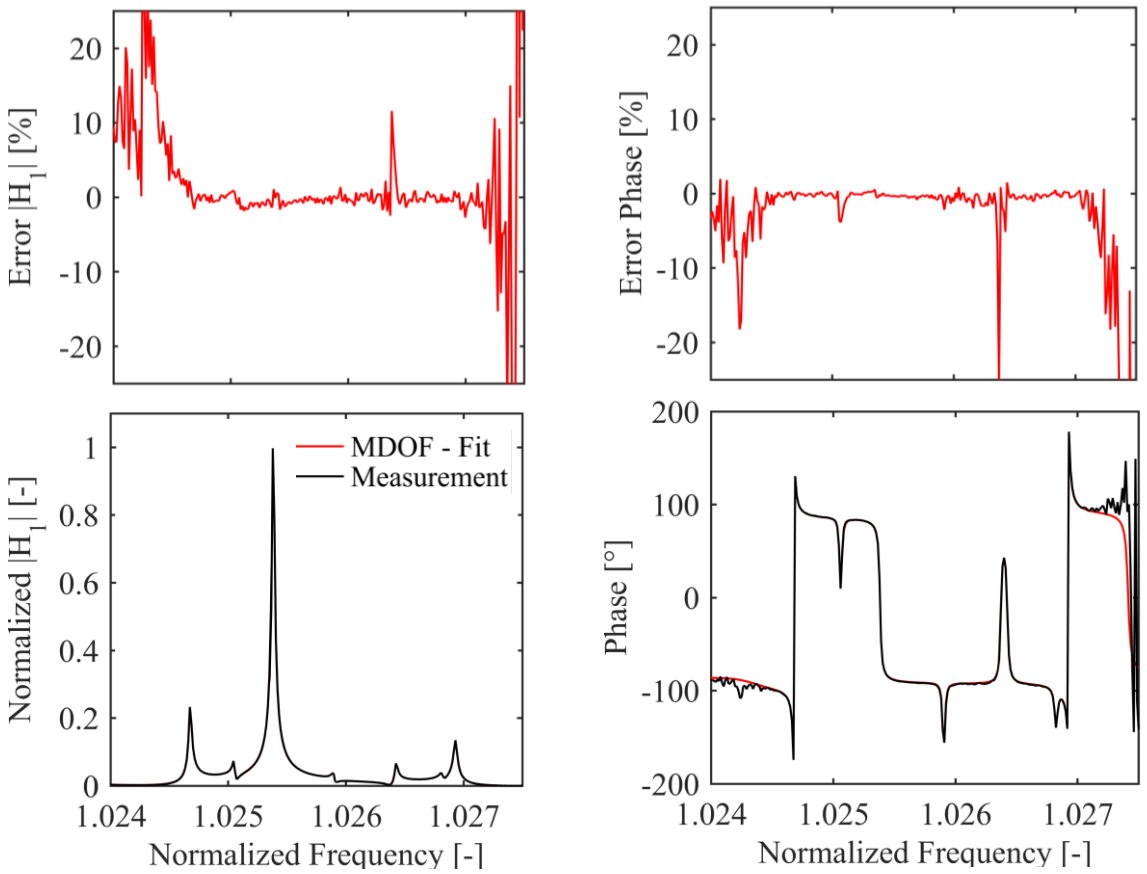

Figure 14: Comparison of measured and fitted forced response function for an exemplary blade in the frequency range of blade mode family 1

In case of the blade integrated disk rotor which is discussed here the introduced fitting algorithm allows to identify about 250 natural frequencies in the range of blade mode 1 to blade mode 3. Moreover 35 eigenvectors are evaluated within this frequency range. More specifically 21 circumferential system modes of blade mode 1, 6 system modes of blade mode 2 and 8 system modes of blade mode 3 are available for model validation. Each eigenvector considers one measurement degree of freedom per blade (cf. Figure 10). The comparably low number of identified eigenvectors can be explained due to the strong modal coupling of neighboring resonances. For these cases a comprehensive evaluation of eigenvectors is much more difficult than natural frequency identification.

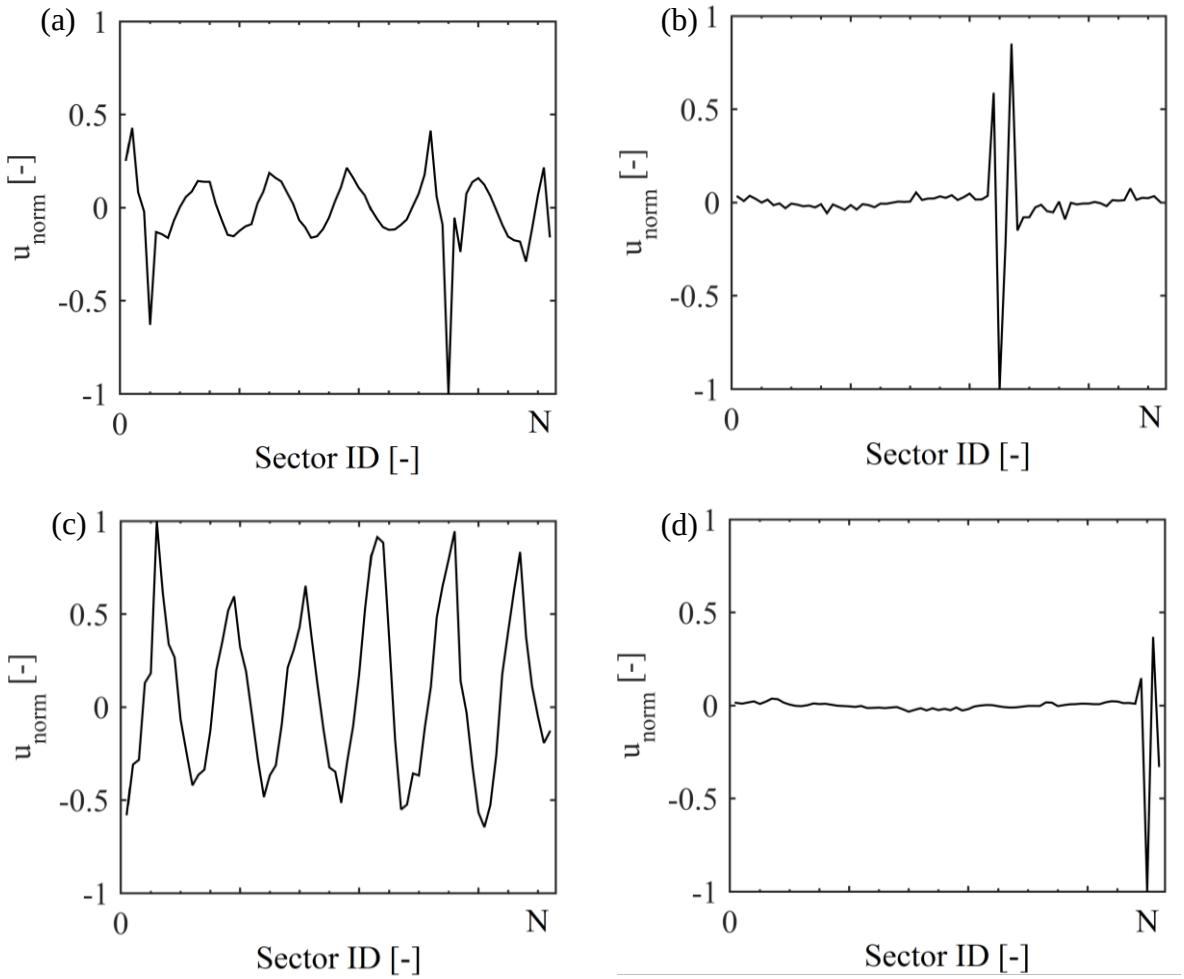

Figure 15: Experimental identified system modes reduced to one degree of freedom (4 modes out of 35)

Figure 15 (a-d) exemplary shows 4 circumferential system modes out of 35 which have been identified within the described measurement campaign. Even this first evaluation of experimental modal analysis impressively demonstrates mistuning effects. Especially modes plotted in Figure 15 (b) and (d) are characterized by a strong localization. That means only a few blades participate in this system mode. In general terms the presented natural frequencies and eigenvectors will be a purposeful data base validating the modified simulation model generated in Chapter 3.

4.3 Validation Results

Key topic of the present paper is to validate geometric modified finite element simulation model. This section uses the modal parameters extracted from vibration measurements as described in Chapter 4.2 and compares them against their numerical counterparts calculated with the finite element model updated in Chapter 3.

First of all the normalized frequencies of the idealized simulation model, the updated simulation model and the experimental identified frequency values are shown in Figure 16(a). The illustration focuses on the frequency range of the first blade mode. Corresponding blade mode shape as well as the circumferential system mode classification has been introduced in Chapter 2. For better understanding a detailed nodal diameter plot is added (Figure 16(b)).

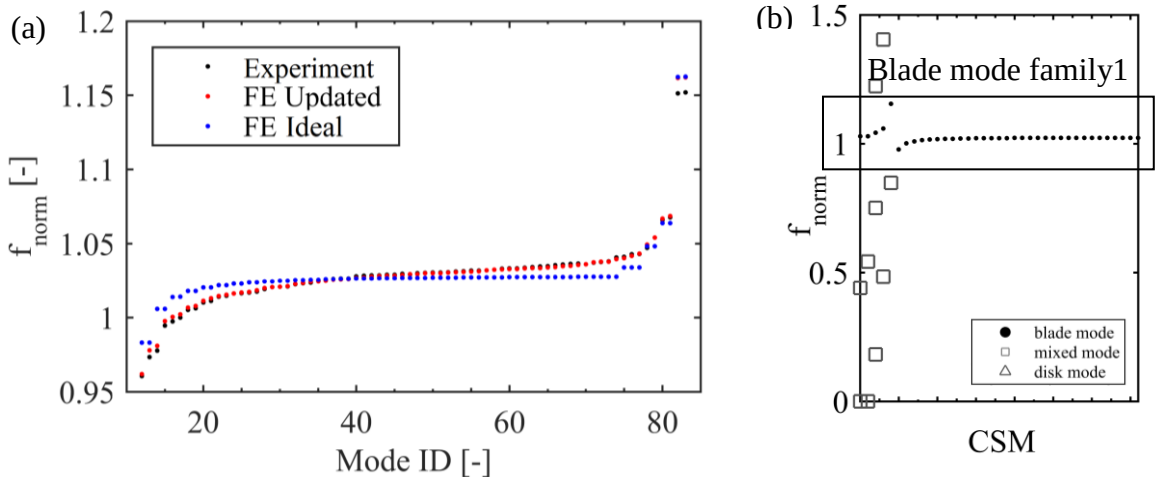

Figure 16: Normalized frequency values in the frequency range of blade mode 1 (a) and the corresponding detailed nodal diameter plot (b)

First of all Figure 16 (a) shows a good match of calculated and measured natural frequencies in case of using the geometry updated finite element model (cf. Chapter 3). Compared with that there are significant deviations in natural frequency prediction comparing the idealized finite element model (cf. Chapter 2) with experimental data. In order to characterize the differences between idealized and updated finite element model towards the experimental identified frequencies a mode individual frequency deviation is introduced

$$df_i = \frac{f_i^{exp/upd} - f_i^{ideal}}{f_i^{ideal}}. \tag{7}$$

Herein f_i^{exp} or f_i^{upd} respectively is the current frequency of interest. Both frequencies are related to the corresponding natural frequency of the idealized finite element model. The resulting deviation plot is presented in Figure 17. As can be seen the first impression of a sufficient model update is confirmed. Deviation characteristics of updated model and experimental data regarding the idealized reference model are nearly the same. In case of blade mode 1 frequency deviations up to 2.5 % are identified comparing the real rotor and the idealized finite element model. Same magnitude is predicted by the updated simulation model. Largest differences between measured and numerically predicted frequency characteristics occur in case of mode IDs corresponding to lower cyclic symmetry indices as for example $i = 82$ or $i = 83$. The comparably large differences are caused by simulation model update input. As described in Chapter 3 optical measurement results are only available for the blade ring section. That means geometric properties of the disk remain unchanged. This obviously influences structur-

al behavior in case of lower cyclic symmetry indices. Further it has to be mentioned that the resonances i = 70 and i = 79 could not be identified by vibration measurements. Because of that it is not possible to calculate the corresponding deviation values df_i.

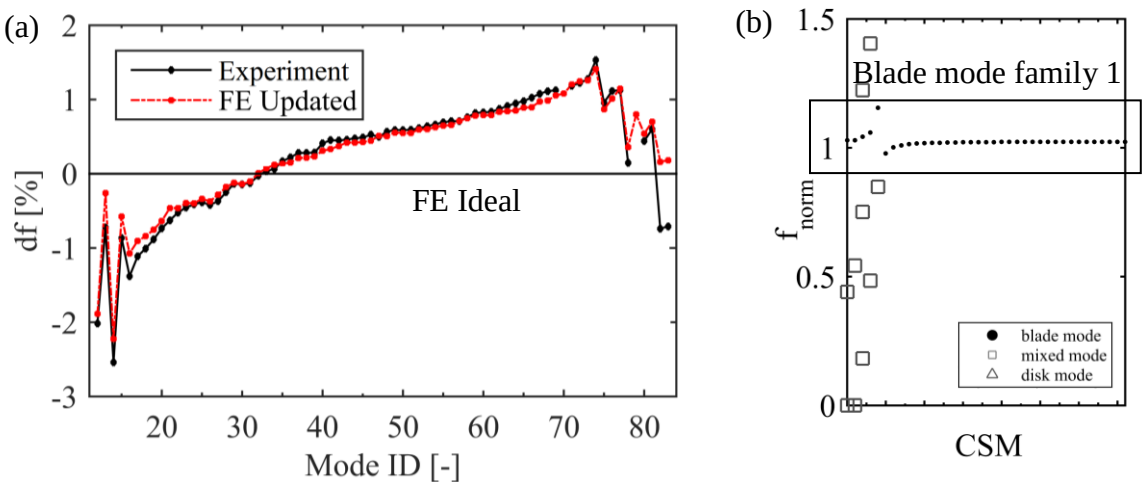

Figure 17: Deviations in natural frequencies between experiment, updated FE and idealized FE model in the frequency range of blade mode family 1 (a) and the corresponding detailed nodal diameter plot (b)

The model validation should be done for a comparable large frequency range. Thus, an identical frequency comparison has been carried out for blade mode 2 and blade mode 3 respectively. In case of blade mode 2 (Figure 18) the impressions of blade mode 1 evaluation are largely confirmed. The frequency deviation characteristics are predicted well by the updated simulation model. Only lower cyclic symmetry indices show comparably large differences.

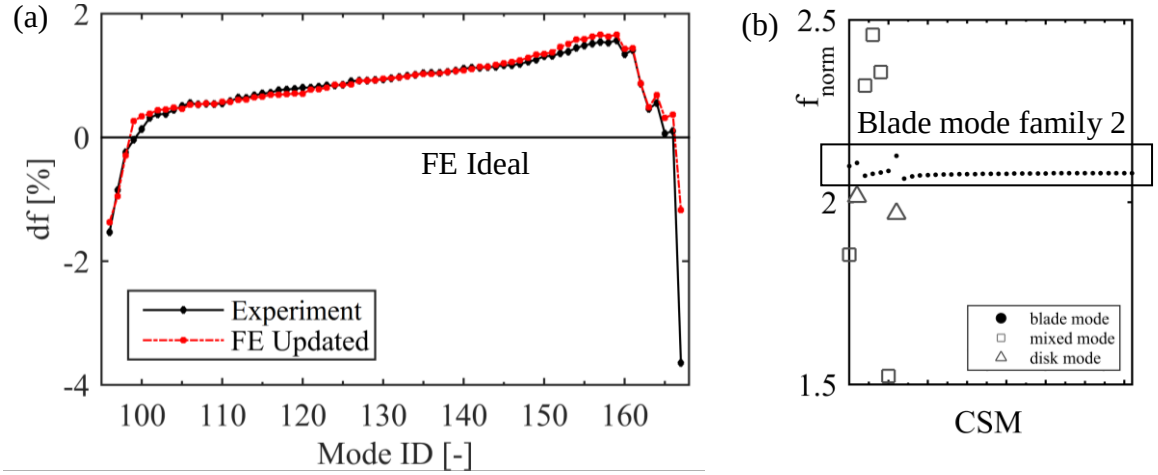

Figure 18: Deviations in natural frequencies between experiment, updated FE and idealized FE model in the frequency range of blade mode family 2 (a) and the corresponding detailed nodal diameter plot (b)

Finally a look at the evaluation results in the frequency range of blade mode 3 (Figure 19) generally confirms previous statements. In detail increasing differences between real blisk and updated simulation model can be observed for resonance IDs higher than i=260. In this context it has to be expected that the occurring differences between measurement results and up-

dated model are increasing by an increasing mode shape complexity. At this point a further discussion is necessary in order to quantify the influence of geometric errors caused by optical measurements. Further it has to be discussed if the finite element mesh is able to represent all relevant geometric features as accurate as necessary. A sufficient mesh study of the ideal model does not necessarily remain valid in case of local geometric deviations.

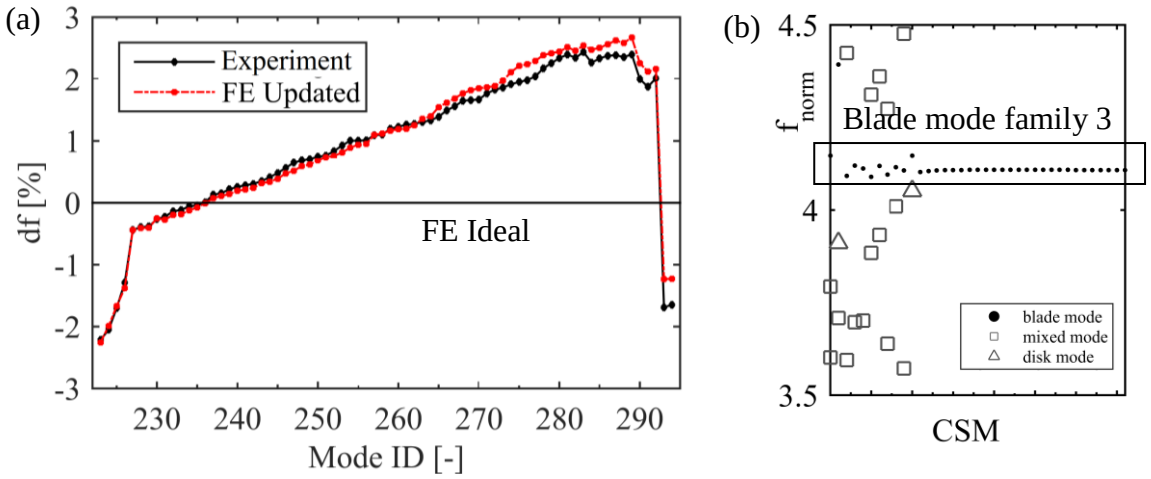

Figure 19: Deviations in natural frequencies between experiment, updated FE and idealized FE model in the frequency range of blade mode family 3 (a) and the corresponding detailed nodal diameter plot (b)

To complete model validation experimentally identified and numerically predicted system modes have to be compared using the Modal Assurance Criterion. As introduced in Chapter 4.2 a system mode is reduced to one degree of freedom per blade. In order to compare numerical and experimental results the numerical based evaluation of the deflection shape is reduced to one node per blade. It has been proven that the position tolerance between simulation model node and real part measurement point has a negligible influence to the resulting circumferential system mode. In the following the conventional MAC is described by

$$\mathrm{MAC}_{\mathrm{exp,fe}} = \frac{(\varphi_{\mathrm{exp}}^{\mathrm{T}}\varphi_{\mathrm{fe}})(\varphi_{\mathrm{fe}}^{\mathrm{T}}\varphi_{\mathrm{exp}})}{(\varphi_{\mathrm{exp}}^{\mathrm{T}}\varphi_{\mathrm{exp}})(\varphi_{\mathrm{fe}}^{\mathrm{T}}\varphi_{\mathrm{fe}})}. \tag{8}$$

In this connection φ is the current eigenvector of interest with one degree of freedom per blade. The main diagonal values of the resulting MAC matrix are shown in the bar chart of Figure 20 (a). It can be seen that the major number of modes is predicted well by the updated simulation model. Only 7 out of 35 modes show diagonal MAC values lower than 0.8. Correlation values for these suboptimal matching circumferential system modes ranging between 0.5 and 0.8. Figure 20 (d-e) exemplary shows three good matching system modes ID = 76, ID = 166 and ID = 224 as well as one suboptimal matching system mode ID = 16.

In order to rate this result the MAC is calculated a second time with the circumferential system modes of the idealized finite element model (cf. Chapter 2). Such a comparison shows nearly no correlation between the tuned finite element model and the measured modes of the real system. Only 5 out of 35 modes have diagonal MAC values greater than 0.5. Thus the efficiency of the model update procedure presented in Chapter 3 is emphasized.

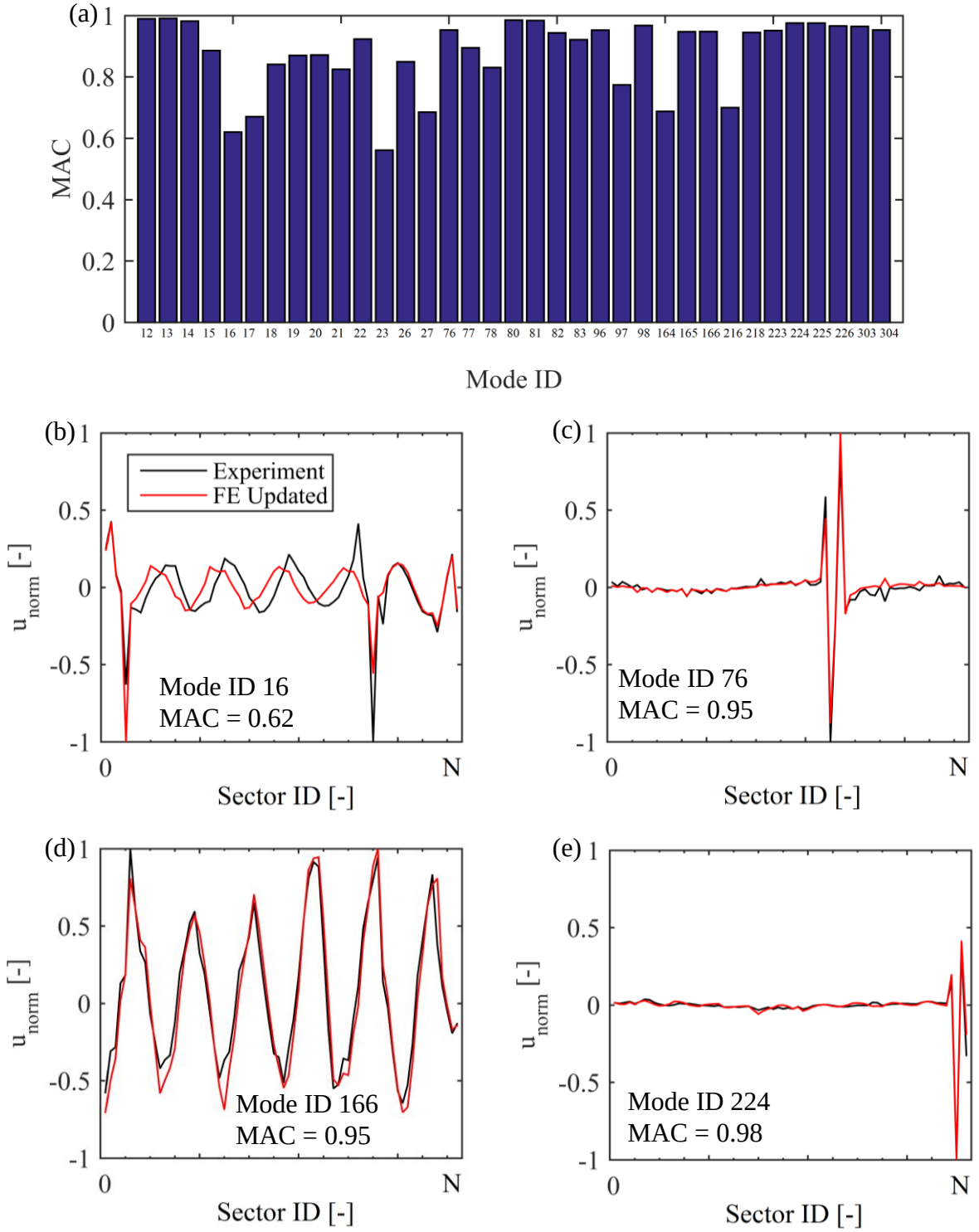

Figure 20: Modal Assurance Criterion for 35 circumferential system modes (a) and detailed comparison of 4 exemplary modes out of 35 (d-e)

Of course the introduced mode shape validation is not that comprehensive as the comparison of natural frequencies. The reasons for that are already discussed in Chapter 4.2. But nevertheless it becomes clear that geometric modifications of blisk simulation models are a sufficient way improving the prediction of structural dynamics behavior.

5 CONCLUSIONS

A finite element model of an idealized blade integrated disk has been introduced and its natural frequencies and mode shapes have been calculated. Within the next step the finite element model was updated using optical measurement data. In order to validate the updated model an experimental setup was presented which was used to identify modal parameters of the real blisk. Vacuum conditions have been proven advantageous in order to get validation data. Largely eliminated aerodynamic damping contribution of the surrounding fluid leads to a much better separation of resonance peaks and the number of evaluable natural frequencies increases dramatically. This finally results in a much more meaningful model validation.

Comparing the experimental identified model parameters with those of the geometric mistuned simulation model leads to the conclusion that geometric modifications of blisk simulation models are a sufficient way improving the prediction of structural dynamics behavior of these components. In this context the presented industrial test blisk has been successfully validated for fundamental blade mode families 1 to 3.

Nevertheless there are several topics which have to be addressed in future research work. From the numerical point of view it is not finally clear which criterion should be used to evaluate the suitability of a finite element mesh in order to consider all geometric features of interest. Furthermore it has to be discussed how to deal with unavoidable measurement errors in context of an optical surface capturing. In addition the vibration measurement setup has to be improved. Here a similarly comprehensive evaluation would be desirable for circumferential system modes as natural frequencies. Alternatively equivalent model validation procedures could be studied for reducing experimental efforts.

6 ACKNOWLEDGMENT

The work presented in this paper is part of the research project ’COOREFLEX-Turbo (Subproject 1.3.4: Robustness Analysis of Blade Vibration)’ which is funded by the German Federal Ministry of Economics and Technology (FKZ 03ET7021). The authors gratefully acknowledge this financial support. Furthermore the authors are grateful to Rolls-Royce Deutschland Ltd & Co KG for granting permission for its publication. Martin Burk, Joerg Weigand, Thomas Stopp and Martin Harding from Rolls-Royce Deutschland Ltd & Co KG in Oberursel are greatly acknowledged for supporting this work by providing the blisk hardware and optical measurement results.

REFERENCES

[1] D.S. Whitehead, Effect of Mistuning on the Vibration of Turbomachine Blades Induced by Wakes, *Journal Mechanical Engineering Science*, Vol. 8, pp. 15-21, 1966.

[2] S.-T. Wei, C. Pierre, Localization Phenomena in Mistuned Assemblies with Cyclic Symmetry Part I: Free Vibrations, *ASME Journal of Vibration, Acoustics, Stress, and Reliability in Design*, 110, pp. 429-438, 1988.

[3] S.-T. Wei, C. Pierre, Localization Phenomena in Mistuned Assemblies with Cyclic Symmetry Part II: Forced Vibrations, *ASME Journal of Vibration, Acoustics, Stress, and Reliability in Design*, 110, pp. 439-449, 1988.

[4] E. P. Petrov, D. J. Ewins, Analysis of the Worst Mistuning Patterns in Bladed Disk Assemblies, *Journal of Turbomachinery*, 125, pp. 623-631, 2003.

[5] J. Jugde, C. Pierre, O. Mehmed, Experimental Investigation of Mode Localization and Forced Response Amplitude Magnification for a Mistuned Bladed Disk, *Journal of Engineering for Gas Turbines and Power*, 123, pp. 940-950, 2001.

[6] M. P.Castanier, C Pierre, Modelling and Analysis of Mistuned Bladed Disk Vibration: Status and Emerging Directions, *Journal of Propulsion and Power*, 22, No. 2, pp. 384-396, 2006.

[7] D. Laxalde, F. Thouverez, J.-J Sinou, J.-P. Lombard, S. Baumhauer, Mistuning Identification and Model Updating of an Industrial Blisk (review Article), *International Journal of Rotating Machinery*, Volume 2007, Article ID 17289, 2007.

[8] D. M. Feiner, J. H. Griffin, Mistuning Identification of Bladed Disks Using a Fundamental Mistuning Model—Part I: Theory, *Journal of Turbomachinery*, 126, pp. 150-158, 2004.

[9] J. A. Judge, C. Pierre, S. L. Ceccio, Experimental mistuning identification in bladed disks using a component-mode-based reduced-order model. *AIAA journal*, *47*(5), 1277-1287, 2009.

[10] H. Schoenenborn, D. Grossmann, W. Satzger & H. Zisik, Determination of blade-alone frequencies of a blisk for mistuning analysis based on optical measurements. In *ASME Turbo Expo 2009: Power for Land, Sea, and Air* (pp. 221-229). American Society of Mechanical Engineers, 2009.

[11] A. A. Kaszynski, J. A. Beck, & J. M Brown. Automated Finite Element Model Mesh Updating Scheme Applicable to Mistuning Analysis. In *ASME Turbo Expo 2014: Turbine Technical Conference and Exposition* (pp. V07BT33A025-V07BT33A025). American Society of Mechanical Engineers, 2014.

[12] V. Ganine, M. Legrand, H. Michalska, & C. Pierre. A sparse preconditioned iterative method for vibration analysis of geometrically mistuned bladed disks. *Computers & Structures*, *87*(5), 342-354, 2009.

[13] D. L. Harris. Measurement of damping of composite materials for turbomachinery applications. *MSFC Center Director's Fund Final Report, Project*, (94-05) ,1998.

[14] J. J. Kielb, & R. S. Abhari. Experimental study of aerodynamic and structural damping in a full-scale rotating turbine. In *ASME Turbo Expo 2001: Power for Land, Sea, and Air* (pp. V004T03A028-V004T03A028). American Society of Mechanical Engineers, 2001, June.

[15] P. Hönisch, A. Kühhorn, & B. Beirow. Experimental and numerical analyses of radial turbine blisks with regard to mistuning. In *ASME 2011 Turbo Expo: Turbine Technical Conference and Exposition* (pp. 971-980). American Society of Mechanical Engineers, 2011, January.

[16] W. Heylen, & T. Janter. Extensions of the modal assurance criterion. *Journal of Vibration and Acoustics*, *112*(4), 468-472, 1990.

[17] K. Harding. Latest optical methods for industrial dimensional metrology. *In Optics East 2005* (pp. 600001-600001). International Society for Optics and Photonics, 2005.

[18] A. A., Kaszynski, J. A. Beck, J. M. Brown. Uncertainties of an automated optical 3d geometry measurement, modeling, and analysis process for mistuned integrally bladed

rotor reverse engineering. *Journal of Engineering for Gas Turbines and Power*, *135*(10), 102504, 2013.

[19] F. Remondino, & S. El-Hakim. Image-based 3D Modelling: A Review. *The Photogrammetric Record*, *21*(115), 269-291, 2006.

[20] B. Beirow, T. Maywald, F. Figaschewsky, C. R. Heinrich, A. Kühhorn, & T. Giersch. Simplified determination of aerodynamic damping for bladed rotors. Part 1: Experimental validation at rest. In *ASME 2016 Turbo Expo: Turbine Technical Conference and Exposition*. American Society of Mechanical Engineers, 2016, June.